Molecular Conductors from Neutral-Radical Charge-Transfer Salts: Preparation and Characterization of an Iodine-Doped Hexagonal Phase of 1,2,3,5-Dithiadiazolyl ($[HCN_2S_2]^\bullet$)

C. D. Bryan,[1a] A. W. Cordes,*[1a] R. C. Haddon,*[1b] R. G. Hicks,[1c] D. K. Kennepohl,[1c] C. D. MacKinnon,[1c] R. T. Oakley,*[1c] T. T. M. Palstra,[1b] A. S. Perel,[1b] S. R. Scott,[1c] L. F. Schneemeyer,[1b] and J. V. Waszczak[1b]

Contribution from the Department of Chemistry and Biochemistry, University of Arkansas, Fayetteville, Arkansas 72701, AT&T Bell Laboratories, 600 Mountain Avenue, Murray Hill, New Jersey 07974, Guelph-Waterloo Centre for Graduate Work in Chemistry, Guelph Campus, Department of Chemistry and Biochemistry, University of Guelph, Guelph, Ontario N1G 2W1, Canada

Received July 28, 1993. Revised Manuscript Received November 30, 1993®

Abstract: Sublimation of 1,2,3,5-dithiadiazolyl *in vacuo* affords a triclinic phase of the dimer $[HCN_2S_2]_2$. The crystals belong to the space group $P\bar{1}$, a = 6.816(3), b = 13.940(2), c = 14.403(3) Å, α = 116.830(14), β = 98.64(3), γ = 99.18(3)°, FW = 212.4 (for $[HCN_2S_2]_2 \cdot [N_2]_{0.08}$), Z = 6. The crystal structure consists of stacked dimers, with three dimers per asymmetric unit. Pairs of asymmetric units, related by an inversion center, generate a pinwheel motif consisting of six dimers. The columnar structure associated with these pinwheels forms close-packed sets of "molecular tubes". Cosublimation of the radical in the presence of iodine in the mole ratio (HCN_2S_2:I = 5:1) yields an iodine-doped hexagonal phase of composition $[HCN_2S_2]_6[I]_{1.1}$. Crystals of this material belong to the space group $P6_1$, $a = b$ = 14.132(16), c = 3.352(5) Å, FW = 128.20, Z = 6. The crystal structure consists of sixfold pinwheels in which the now evenly spaced HCN_2S_2 rings form a spiral about the 6_1 axis. The iodine atoms lie within the columnar cavity of the pinwheels in a disordered array wrapped tightly about the sixfold screw axis. The single-crystal conductivity of the doped material is 15 S cm^{-1} at room temperature. Raman spectroscopic and magnetic susceptibility measurements on the doped material are reported.

Introduction

The most common method for the synthesis of organic conductors involves the oxidation or reduction of a closed-shell molecule to generate a mixed-valence or charge-transfer salt. Donors such as tetrathiafulvalene (TTF), tetramethyltetraselenafulvalene (TMTSF), and BEDT-TTF have found wide application,[2] and acceptors like tetracyanoquinodimethane (TCNQ) and, more recently, C_{60} have also been pursued.[3] We have been interested in an alternative approach, namely the development of materials based on building blocks consisting of neutral π-radicals, in which the requirement for a partially filled energy band is inherently fulfilled. Within this context we have considered several variants[4] of the originally proposed phenalenyl framework[5] and have focused on derivatives of 1,2,3,5-dithiadiazolyl and 1,2,3,5-diselenadiazolyl.[6] Our intent has been to generate crystal structures consisting of one-dimensional stacks or columns, and for several derivatives the desired stacking arrangement has been achieved.[7] By definition, however, a one-dimensional stack of radicals is formally associated with a half-filled energy band and is susceptible to a charge density wave (CDW) driven or Peierls instability. To date we have attempted to stabilize the metallic state by the application of pressure and by preparing compounds in which two- and three-dimensional interactions are enhanced. Several small band gap semiconductors have been characterized.[7]

An alternative approach to the design of conductive materials based on neutral radicals involves p-type doping of the energy band away from the half-filled level associated with the neutral state. We have recently communicated that conductive materials can be generated in this way. The bifunctional radical [1,4-$(S_2N_2C)C_6H_4(CN_2S_2)$],[8] for example, reacts with iodine to form the charge-transfer salt [1,4-$(S_2N_2C)C_6H_4(CN_2S_2)$][I].[9] The solid-state packing of the molecular units in this salt (space group *Immm*) is, however, quite different from that observed in the parent dimer [1,4-$(S_2N_2C)C_6H_4(CN_2S_2)]_2$ (space group $P2_1/n$). We now report an example of a dithiadiazolyl crystal structure

® Abstract published in *Advance ACS Abstracts,* January 15, 1994.

(1) (a) University of Arkansas. (b) AT&T Bell Laboratories. (c) University of Guelph.

(2) See, for example: (a) Garito, A. F.; Heeger, A. J. *Acc. Chem. Res.* **1974**, *7*, 232. (b) Torrance, J. B. *Acc. Chem. Res.* **1979**, *12*, 79. (c) Williams, J. M.; Ferraro, J. R.; Thorn, R. J.; Carlson, K. D.; Geiser, U.; Wang, H. H.; Kini, A. M.; Whangbo, M. H. *Organic Superconductors (Including Fullerenes): Synthesis, Structure, Properties and Theory*; Prentice-Hall: Englewood Cliffs, New Jersey, 1992. (d) Bryce, M. R. *Chem. Soc. Rev.* **1991**, *20*, 355.

(3) (a) Haddon, R. C.; Hebard, A. F.; Rosseinsky, M. J.; Murphy, D. W.; Glarum, S. H.; Palstra, T. T. M., Ramirez, A. P.; Duclos, S. J.; Fleming, R. M.; Siegrist, T.; Tycko, R. *ACS Symp. Ser.* **1992**, *481*, 71. (b) Haddon, R. C. *Acc. Chem. Res.* **1992**, *25*, 127.

(4) (a) Haddon, R. C.; Wudl, F.; Kaplan, M. L.; Marshall, J. H.; Cais, R. E.; Bramwell, F. B. *J. Am. Chem. Soc.* **1978**, *100*, 7629. (b) Kaplan, M. L.; Haddon, R. C.; Hirani, A. M.; Schilling, F. C.; Marshall, J. H. *J. Org. Chem.* **1981**, *46*, 675. (c) Haddon, R. C.; Chichester, S. V.; Stein, S. M.; Marshall, J. H.; Mujsce, A. M. *J. Org. Chem.* **1987**, *52*, 711. (d) Hayes, P. J.; Oakley, R. T.; Cordes, A. W.; Pennington, W. T. *J. Am. Chem. Soc.* **1985**, *107*, 1346. (e) Oakley, R. T.; Reed, R. W.; Cordes, A. W.; Craig, S. L.; Graham, J. B. *J. Am. Chem. Soc.* **1987**, *109*, 7745.

(5) Haddon, R. C. *Nature (London)* **1975**, *256*, 394.

(6) Cordes, A. W.; Haddon, R. C.; Oakley, R. T. In *The Chemistry of Inorganic Ring Systems*; Elsevier: Studel, R., Ed.; Amsterdam, The Netherlands, 1992; p 295.

(7) (a) Cordes, A. W.; Chamchoumis, C. M.; Hicks, R. G.; Oakley, R. T.; Young, K. M.; Haddon, R. C. *Can. J. Chem.* **1992**, *70*, 919. (b) Cordes, A. W.; Haddon, R. C.; Hicks, R. G.; Oakley, R. T.; Palstra, T. T. M. *Inorg. Chem.* **1992**, *31*, 1802. (c) Andrews, M. P.; Cordes, A. W.; Douglass, D. C.; Fleming, R. M.; Glarum, S. H.; Haddon, R. C.; Marsh, P.; Oakley, R. T.; Palstra, T. T. M.; Schneemeyer, L. F.; Trucks, G. W.; Tycko, R.; Waszczak, J. V.; Young, K. M.; Zimmerman, N. M. *J. Am. Chem. Soc.* **1991**, *113*, 3559. (d) Cordes, A. W.; Haddon, R. C.; Hicks, R. G.; Oakley, R. T.; Palstra, T. T. M.; Schneemeyer, L. F.; Waszczak, J. V. *J. Am. Chem. Soc.* **1992**, *114*, 1729. (e) Cordes, A. W.; Haddon, R. C.; Hicks, R. G.; Kennepohl, D. K.; Oakley, R. T.; Palstra, T. T. M.; Schneemeyer, L. F.; Scott, S. R.; Waszczak, J. V. *Chem. Mater.* **1993**, *5*, 820.

(8) Cordes, A. W.; Haddon, R. C.; Oakley, R. T.; Schneemeyer, L. F.; Waszczak, J. V.; Young, K. M.; Zimmerman, N. M. *J. Am. Chem. Soc.* **1991**, *113*, 582.

0002-7863/94/1516-1205$04.50/0

which accepts iodine into the lattice without major changes. This discovery evolved from our recent study of the prototypal 1,2,3,5-dithiadiazolyl $[HCN_2S_2]^\bullet$ (**1**).[10] The crystal structure reported

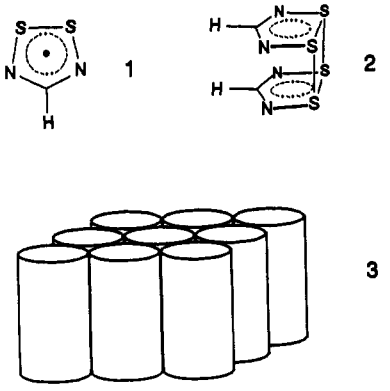

for the radical dimer $[HCN_2S_2]_2$ (**2**) was monoclinic, space group $P2_1/c$, and consisted of stacked columns of dimers, with three dimers in the asymmetric unit. We have now identified a triclinic phase, space group $P\bar{1}$, which also consists of stacked dimers, with three dimers in the asymmetric unit. By contrast, however, this second phase exhibits an unusual tubular structure, e.g., **3**, reminiscent of the hexagonal phase of urea. Since urea is known to form inclusion compounds with many small molecules,[11] it occurred to us that host/guest complexes could also be prepared based on this new phase for $[HCN_2S_2]_2$. We have found that cosublimation of **1** and iodine produces a doped phase, with exact hexagonal symmetry, based on the original triclinic lattice. Herein we describe the preparation and crystal structures of both the triclinic and doped hexagonal phases and report the magnetic and conductivity characteristics of the doped material.

Results

Preparation and Doping of Triclinic $[HCN_2S_2]_2$. In our earlier report of the characterization of the monoclinic phase of $[HCN_2S_2]_2$, we noted that the conditions for crystal growth involved sublimation of the radical under an atmosphere of argon. In practice the samples were heated in sealed tubes subjected to a gentle temperature gradient from 70 to 20 °C. An alternative method for crystal growth, indeed the one most commonly used for bulk sample purification, involves sublimation of the radical *in vacuo* (typically 10^{-2} Torr). Under these pressure conditions a temperature gradient of 30–0 °C (ice/water) is usually employed. The crystalline needles so obtained are thinner, and more fibrous, than those obtained by the 1-atm sublimation, and structural (X-ray) characterization required the selection and preliminary analysis of many crystals. The samples were usually collected after flooding the sublimer with dry nitrogen, and this could account for the inclusion of trace quantities of what may be dinitrogen (*vide infra*) into the lattice.

The reactions of **1** with iodine were carried out in sealed, evacuated tubes. The reagents (either the monoclinic or the triclinic phase of the dimer **2**) were vaporized along a temperature gradient from 70 to 30 °C, and the tube was then reversed and the sublimate re-evaporated. After several (at least six) passes, a relatively homogeneous selection of lustrous silver-black hexagonal crystals was produced. In early experiments the two reagents were introduced in a ratio of 6:1 ($[HCN_2S_2]$:I), but after repeated chemical and crystallographic analyses of the best samples (see Experimental Section), which established the level of loading of iodine in the doped material, the stoichiometry of mixing was eventually adjusted to 5:1. The crystals so obtained were harvested in an argon-filled drybox. Although they are relatively air-sensitive, losing their luster after 2-3 min of exposure, they could be handled for shorter periods in dry air (for X-ray crystal mounting purposes).

Table 1. Atomic Parameters x, y, z, and B_{iso} for Triclinic $[HCN_2S_2]_2 \cdot [N_2]_{0.08}$[a]

	x	y	z	B_{iso}[b]
S1	0.5658(5)	0.35057(23)	0.40156(23)	3.65(17)
S2	0.4344(5)	0.18884(23)	0.28204(23)	3.65(18)
S3	0.1317(5)	0.39332(22)	0.41136(23)	3.65(19)
S4	0.0032(5)	0.23110(23)	0.29256(22)	3.26(17)
S5	0.0955(5)	0.30457(23)	0.07897(22)	3.39(17)
S6	0.1745(5)	0.43236(22)	0.04596(23)	3.28(18)
S7	0.5228(5)	0.25829(23)	0.05802(24)	3.77(19)
S8	0.5966(5)	0.38717(23)	0.02443(21)	3.29(17)
S9	0.1728(5)	−0.10092(25)	0.20578(23)	3.50(19)
S10	0.2454(5)	−0.06821(24)	0.36342(23)	3.31(17)
S11	−0.2552(5)	−0.05519(23)	0.22651(22)	3.40(19)
S12	−0.1814(5)	−0.02195(22)	0.38431(21)	3.10(17)
N1	0.5694(16)	0.3227(8)	0.5020(7)	3.6(6)
N2	0.4147(14)	0.1386(7)	0.3635(8)	3.7(6)
N3	0.1158(16)	0.3693(8)	0.5014(7)	4.2(6)
N4	−0.0276(15)	0.1829(7)	0.3757(7)	3.7(6)
N5	0.1843(15)	0.3831(7)	0.2111(6)	3.6(6)
N6	0.2765(16)	0.5259(7)	0.1697(7)	4.0(6)
N7	0.6227(15)	0.3333(8)	0.1871(7)	4.1(6)
N8	0.7078(14)	0.4814(7)	0.1496(7)	3.5(6)
N9	0.0625(16)	−0.2338(7)	0.1549(7)	4.1(6)
N10	0.1507(15)	−0.1967(7)	0.3343(8)	3.8(6)
N11	−0.3639(14)	−0.1874(7)	0.1776(7)	3.2(6)
N12	−0.2829(16)	−0.1493(7)	0.3568(7)	3.5(6)
C1	0.4865(18)	0.2152(11)	0.4665(10)	3.6(7)
C2	0.0365(22)	0.2617(11)	0.4764(10)	4.1(8)
C3	0.2661(19)	0.4891(10)	0.2401(9)	3.9(7)
C4	0.7046(20)	0.4388(11)	0.2140(10)	4.0(8)
C5	0.0650(18)	−0.2637(8)	0.2306(9)	3.4(6)
C6	−0.3602(18)	−0.2165(8)	0.2544(10)	3.4(7)
N98	0.08570	0.0	0.0	3.6
N99	0.25150	0.0	0.0	3.6
H1	0.478	0.192	0.519	4.6
H2	0.026	0.240	0.530	5.1
H3	0.319	0.541	0.315	4.2
H4	0.767	0.488	0.288	4.7
H5	0.000	−0.339	0.208	3.6
H6	−0.419	−0.292	0.232	4.4

[a] Estimated standard deviations (ESDs) refer to the last digit printed. [b] B_{iso} is the mean of the principal axes of the thermal ellipsoid.

Crystal Structure of Triclinic $[HCN_2S_2]_2$. Atomic coordinates for the triclinic phase of $[HCN_2S_2]_2$ are provided in Table 1, and a summary of pertinent bond lengths is presented in Table 2. Like the case of monoclinic phase, the structure of the triclinic phase also consists of stacked dimers, with three dimers in the asymmetric unit. Figure 1 illustrates the stacking of the asymmetric units in the x direction. The intradimer S–S distance (mean 3.103 Å), and the interdimer S- - -S contacts along the stack (mean 3.786 Å) are comparable to those seen in the monoclinic structure. The internal ring bonds and angles are also very similar.

The major difference between the two phases can be appreciated when the two structures are viewed down the stacking direction. In both the triclinic and monoclinic phases the stacks associate into groups of six, each comprised of two centrosymmetrically related sets of the three crystallographically independent dimers. In the monoclinic crystal these six-stack groups have an irregular cross section which represents efficient space filling.[10] By contrast the six-stack groups of the triclinic phase resemble a pinwheel or "merry-go-round" motif (Figure 2). The three-dimensional structure thus consists of a series of molecular tubes, inside of which there is a strikingly large cavity. In the refinement of the

(9) Bryan, C. D.; Cordes, A. W.; Fleming, R. M.; George, N. A.; Glarum, S. H.; Haddon, R. C.; Oakley, R. T.; Palstra, T. T. M.; Perel, A. S.; Schneemeyer, L. F.; Waszczak, J. V. *Nature (London)* **1993**, *365*, 821.

(10) Cordes, A. W.; Bryan, C. D.; Davis W. M.; DeLaat, R. H.; Glarum, S. H.; Goddard, J. D.; Haddon, R. C.; Hicks, R. G.; Kennepohl, D. K.; Oakley, R. T.; Scott, S. R.; Westwood, N. P. C. *J. Am. Chem. Soc.* **1993**, *115*, 7232.

(11) Takemoto, K.; Sonoda, N. *Inclusion Compounds of Urea, Thiourea and Selenourea*; Academic Press: London, 1984; p 47.

Table 2. Summary of Intra- and Intermolecular S–S Distances[a] (Å)

Triclinic $[HCN_2S_2]_2 \cdot [N_2]_{0.08}$					
Intramolecular					
S–S	2.062(15)	S–N	1.636(35)	C–N	1.326(37)
stack A		stack B		stack C	
Intradimer					
S1–S3	3.121(5)	S5–S7	3.111(5)	S9–S11	3.113(5)
S2–S4	3.101(5)	S6–S8	3.073(5)	S10–S12	3.107(5)
Interdimer Contacts along Stack					
S1-S3′	3.779(5)	S5-S7′	3.796(5)	S9-S11′	3.792(5)
S2-S4′	3.797(5)	S6-S8′	3.830(5)	S10-S12′	3.800(5)
Interdimer Contacts around Pinwheel					
S9-S2	3.716(4)	S2-S7	3.864(4)	S7-S11′	3.711(4)
S11-S4	3.710(4)	S4-S5	3.759(4)	S5-S9′	3.715(4)
Interdimer Contacts between Columns					
S1-S3′ at *a*		3.400(4)		($a = 1-x, 1-y, 1-z$)	
S6-S8′ at *b*		3.364(4)		($b = 1-x, 1-y, -z$)	
S10-S12′ at *c*		3.391(4)		($c = -x, -y, 1 = z$)	
S12-S12′ at *c*		3.577(6)			
Hexagonal $[HCN_2S_2]_6[I]_{1.1}$					
Intramolecular					
S–S	2.051(11)	S–N	1.65(3)	C–N	1.33(4)
Interannular Contacts around Pinwheel					
S2-S2′			3.742(21)		
Interannular Contacts between Columns					
S1-S1′			3.490(13)		

[a] Numbers in parentheses are ESDs for single-valued distances. For averaged distances, the number is the greater of the range and ESD. Primes designate atoms in a different asymmetric unit.

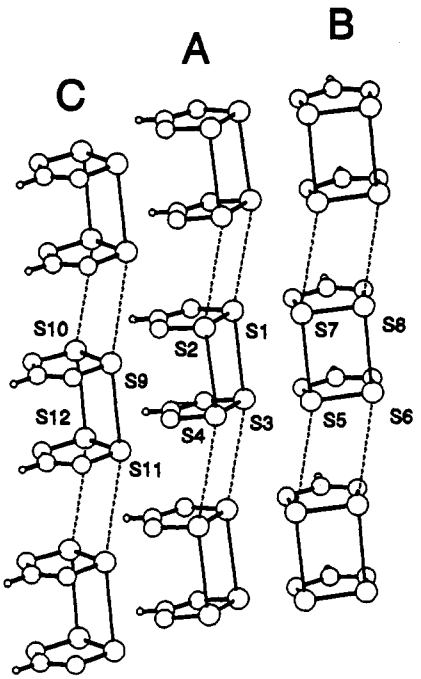

Figure 1. Stacking of dimer units in the triclinic phase of **2**. The three columns in the asymmetric unit are denoted as A, B, and C.

structure two centers of electron density were located within these tubes and were eventually modeled by nitrogen atoms with fractional occupancies (see Experimental Section). The size of the columnar cavity can be estimated in terms of the perpendicular distances of the innermost sulfur atoms of the three dimer units to the $\bar{1}$ axis; these values range from a low of 3.309 Å (for S7) to a high of 3.985 Å (S4) with an average of 3.715 Å; the average diameter of the cavity is thus 7.43 Å. The molecular tubes are locked in a close-packed arrangement, e.g., **3**, which constitutes a near-hexagonal crystal symmetry. Three series of close S- - -S

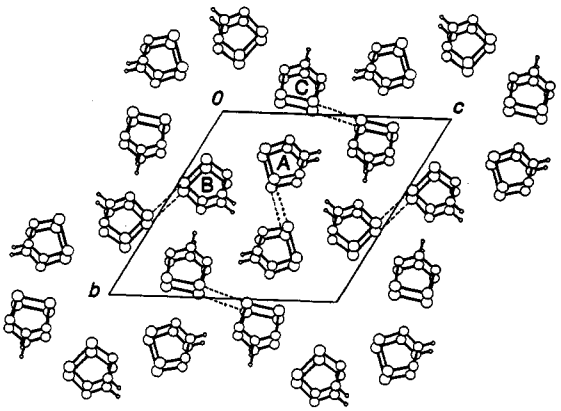

Figure 2. View of packing of the triclinic phase of **2** in the *yz* plane. The three dimers in the asymmetric unit are denoted as A, B, and C. Intercolumnar S- - -S contacts are shown with dashed lines.

Table 3. Atomic Parameters *x*, *y*, *z*, and B_{iso} for hexagonal $[HCN_2S_2]_6[I]_{1.1}$[a]

	x	*y*	*z*	B_{iso}[b]
S1	0.3784(6)	0.4139(6)	0.00000	6.5(5)
S2	0.2188(7)	0.2901(7)	0.012(4)	7.1(5)
N1	0.3498(21)	0.5138(19)	0.008(9)	6.9(6)
N2	0.1665(16)	0.3715(18)	0.047(11)	6.9(6)
C1	0.242(3)	0.4749(25)	0.064(12)	8.9(9)
H1	0.2175	0.5257	0.0880	9.57
I1[c]	0.95921	0.94785	0.02802	7.08
I2[c]	0.97626	0.99258	0.86319	1.89

[a] ESDs refer to the last digit printed. [b] B_{iso} is the mean of the principal axes of the thermal ellipsoid. [c] Occupancy factor for I1 is 0.065 and for I2 is 0.116.

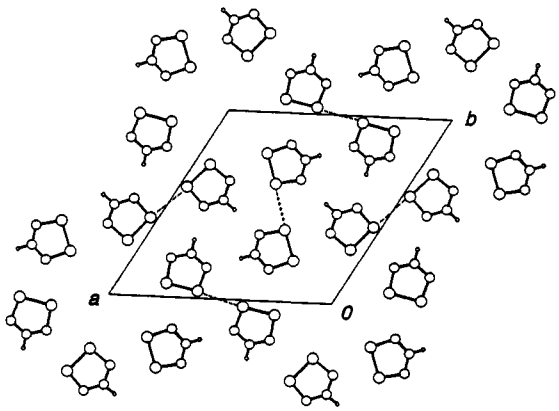

Figure 3. View of packing of the hexagonal iodine-doped phase in the *xy* plane. The iodine atoms are omitted for clarity. Intercolumnar S- - -S contacts are shown with dashed lines.

intercolumnar contacts, indicated in Figure 2 and enumerated in Table 2, link the tubes together.

Crystal Structure of $[HCN_2S_2]_6[I]_{1.1}$ Crystals of the doped material belong to the polar hexagonal space group $P6_1$. Atomic coordinates are provided in Table 3, and a summary of pertinent intra- and interannular structural parameters is presented in Table 2. From a molecular perspective, incorporation of iodine into the lattice has virtually no effect on the internal structure of the HCN_2S_2 ring. As in the parent triclinic phase of the radical dimer, the crystal structure consists of molecular tubes, each tube being composed of a pinwheel array of six HCN_2S_2 rings, as shown in Figure 3; intercolumnar contacts are defined in Table 2. As a result of the crystallographic symmetry, the arrangement of the tubes is now perfectly close-packed, and the rings within each pinwheel are related by a sixfold screw axis through the center of the pinwheel. The principal differences between the stacking of the parent triclinic phase and that of the doped hexagonal phase are illustrated in Figure 4. The most notable

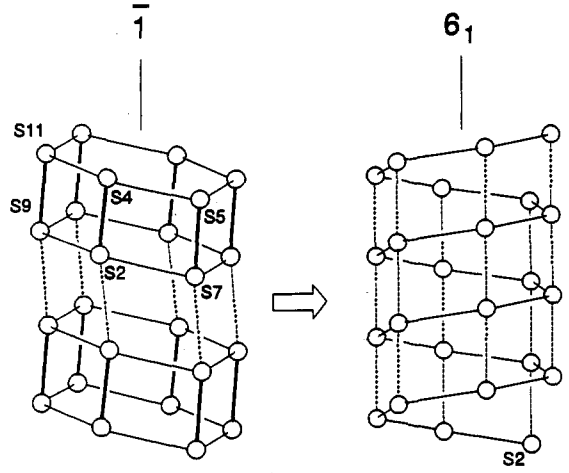

Figure 4. Internal rearrangement of columnar cavities in $[HCN_2S_2]_2$ occasioned by iodine doping. The nearly horizontal connectivity lines on the left, and the spiral connectivity lines on the right, are defined in Table 2.

feature of the doped structure is the molecular repeat distance, the unit cell dimension α, which is now 3.352(5) Å, i.e., the heterocyclic HCN_2S_2 rings are uniformly spaced. The internal diameter of the tubes, defined as twice the distance from the innermost sulfur (S2) to the 6_1 axis, is 7.40 Å, i.e., very similar to that observed in the undoped structure.

Iodine atoms are incorporated into the columnar cavities and are disordered. The disorder model presented here essentially distributes the electron density of the iodines evenly along the cavities. The 6_1 symmetry, the 3.352 Å cell repeat, and the sites used give a tight spiral of iodine positions which are separated by about 0.5 Å both horizontally and vertically, with a spiral diameter of less than 1 Å. Many crystals of this material were examined, and a total of four data sets were collected. The data and the iodine occupancies presented here are from the best refinement. In the other data sets the occupancy varied from a low of 0.18 to a high of 0.22. The reported value corresponds to an iodine loading of 1.1 iodines per six $[HCN_2S_2]$ units and is in good agreement with the results of repeated chemical analyses on different samples.

Raman Spectra of $[HCN_2S_2]_2$ and $[HCN_2S_2]_6[I]_{1.1}$ In order to probe further the structural changes associated with iodine incorporation, we have recorded the Raman spectra of the parent compound $[HCN_2S_2]_2$ (triclinic phase) and its iodine-doped derivative $[HCN_2S_2]_6[I]_{1.1}$ (Figure 5). In the undoped material, clear, well-resolved bands are observed throughout the entire vibrational region; a complete listing of the observed Raman bands is provided in the Experimental Section.[12] For the doped material, however, scattering associated with iodine dominates the spectrum, and only two broad bands, at 107 and 148 cm^{-1}, are observed. In the undoped compound the most notable feature, within the present context, is the strong, broad band centered at 124 cm^{-1}. In our recent analysis of the gas-phase vibrational spectrum of $[HCN_2S_2]^\bullet$ (**1**), we determined (from *ab initio* frequency calculations) that the lowest vibrational modes should occur near 475 cm^{-1} (A_1 symmetry) and 219 cm^{-1} (A_2 symmetry).[10] Of these, the former, which is loosely associated with the internal S–S bond, is predicted to be very strong in the Raman spectrum; the latter is predicted to be vanishingly weak.[13] Dimerization of the radical perturbs the gas-phase structure only slightly,[10] from which we conclude that the observed band at 463 cm^{-1} in triclinic $[HCN_2S_2]_2$ is still largely an intra-annular S–S stretch. Because

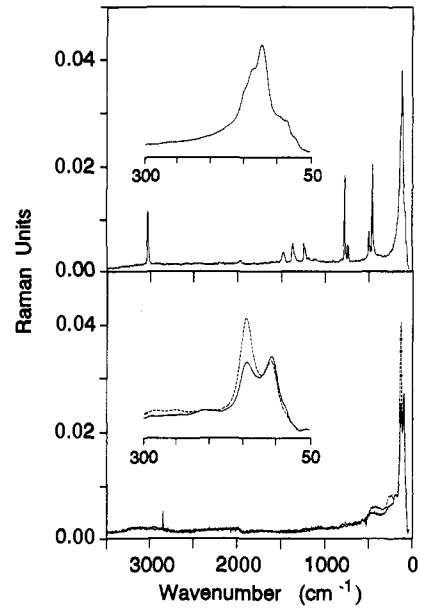

Figure 5. Raman spectra of triclinic $[HCN_2S_2]_2$ (above) and $[HCN_2S_2]_6[I]_{1.1}$ (below). Inserts are magnifications of the 300–50-cm^{-1} region. For the doped material two temperatures are shown: 295 K (solid line) and 130 K (dashed line). The spike near 2800 cm^{-1} in the lower spectrum is of instrumental origin.

there are no predicted Raman-active intra-annular modes below the 400-cm^{-1} region, we assign the band centered at 124 cm^{-1} to interannular S- - -S vibrations which are broadened by lattice coupling effects. We do not, however, venture beyond qualitative assignments of the two Raman bands in $[HCN_2S_2]_6[I]_{1.1}$. One or both may involve the internal stretching modes of a linear polyiodide species.[14] In benzophenone/iodine/potassium iodide (BIKI),[15] for example, the disordered iodines also occupy a hexagonal cavity,[16] and the resonance Raman spectrum displays broad bands at 167 and 108 cm^{-1}.[17] However, the possibility that weak S- - -S or even S- - -I interactions are involved in the present system cannot be discounted.

In spite of these uncertainties surrounding the low-frequency region, we can conclude that at both room (295 K) and low (130 K) temperature there is partial charge transfer from iodine to radical, i.e., the encapsulated iodine is in the form of a polyiodide. We refrain, however, from formal assessment of the degree of charge transfer. The subtle changes observed on cooling the doped material, i.e., the increase in the intensity of the higher frequency band, may be indicative of a subtle change in charge transfer and may also signal the onset of some association of the rings (see the magnetic measurements below).

Magnetic and Conductivity Measurements. The measured magnetic susceptibility of $[HCN_2S_2]_6[I]_{1.1}$ as a function of temperature is shown in Figure 6. As in the case of $[1,4\text{-}(S_2N_2C)\text{-}C_6H_4(CN_2S_2)][I]$,[9] the concentration of spin-bearing defects is very low (0.01% per molecule), and at low temperatures the material is diamagnetic (confirmed by ESR). A pronounced spin susceptibility beings to develop at about 180 K, and the sample paramagnetism continues to increase to the highest temperatures attainable (before sample decomposition). Similar behavior was seen for $[1,4\text{-}(S_2N_2C)C_6H_4(CN_2S_2)][I]$, except that in that case the rise in susceptibility slowed above room

(12) We find no Raman evidence for any occluded N_2 in the undoped material.

(13) The relative Raman activities (6-31G**) of the calculated bands at 475 and 219 cm^{-1} are 31.6 and 0.006, respectively. Goddard, J. D. Personal communication.

(14) (a) Marks, T. J.; Kalina, D. W. *Ext. Linear Chain Compd.* **1982**, *1*, 197. (b) Coppens, P. *Ext. Linear Chain Compd.* **1982**, *1*, 333.

(15) Coppens, P.; Leung, P. C. W.; Ortega, R.; Young, W. S.; Laporta, C. *J. Phys. Chem.* **1983**, *87*, 3355.

(16) In BIKI the iodine species has been modeled by a unit consisting of coupled I_3^- and I_2 molecules in a ratio of 4:3. Overall the I_{18}^{4-} repeat distance has a length of 54.90 Å and corresponds to an average I–I separation of 3.05 Å.

(17) Bolton, B. A.; Prasad, P. N. *Mol. Cryst. Liq. Cryst.* **1981**, *76*, 309.

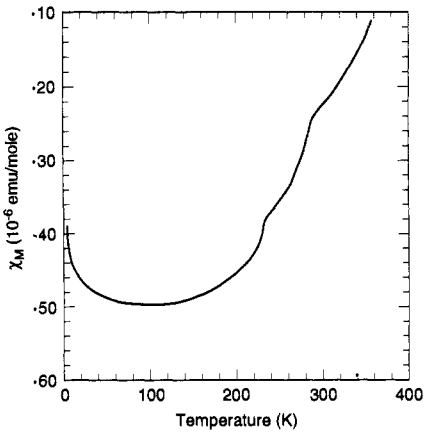

Figure 6. Magnetic susceptibility of $[HCN_2S_2]_6[I]_{1.1}$ as a function of temperature.

temperature.[9] Furthermore, the two inflection points seen in the susceptibility of $[HCN_2S_2]_6[I]_{1.1}$ were not apparent in the magnetic study of [1,4-$(S_2N_2C)C_6H_4(CN_2S_2)$][I]. However, two phase transitions were observed by X-ray diffraction and conductivity studies.[9] It is therefore possible that the points of inflection seen in the magnetic susceptibility of $[HCN_2S_2]_6[I]_{1.1}$ also correspond to transition(s) between metal and charge density wave (CDW) insulator.

The volatility and air sensitivity of $[HCN_2S_2]_6[I]_{1.1}$ have provided a major barrier to a complete single-crystal conductivity measurement. Wires were attached to a number of samples in a He-filled drybox, but the contact and sample degradation were sufficiently rapid to preclude variable-temperature studies. Two samples were measured in a drybox, by using gold paint to attach the leads, and in each case the conductivity was found to be 15 S cm^{-1}.

Summary

In addition to the tetrathiafulvalene-based donors already noted,[2] many other closed-shell molecules, e.g., aromatic hydrocarbons and amines, form conductive charge-transfer compounds with iodine.[14,18,19] In many of these complexes, the crystal structures exhibit linear arrays of disordered iodines, in the form of a complex polyiodide, encapsulated in a channel-like cavity within the host molecular lattice. The present system, however, represents only the second example[9] of a highly conductive material to be generated by the p-type doping of a neutral radical. It is, moreover, a rare example of a molecular conductor which, like C_{60}, retains its basic structure during the doping process (the dopant fills a structural void). In the present case the combination of stoichiometry, cell repeat distance, and Raman spectroscopic data for $[HCN_2S_2]_6[I]_{1.1}$ collectively indicate the presence of a polyiodide in the columnar cavity. Although we cannot fix the degree of charge transfer with any exactitude, the stoichiometry of the material requires that the oxidation state of each HCN_2S_2 ring in the doped compound be less than +0.18.[20]

The sensitivity of the present compound to oxygen and moisture has precluded a detailed analysis of its low-temperature structure and transport properties. From the similarity of the magnetic behavior of $[HCN_2S_2]_6[I]_{1.1}$ and [1,4-$(S_2N_2C)C_6H_4(CN_2S_2)$]-[I],[9] we are nonetheless able to conclude that in the former, as in the latter, a CDW-driven instability sets in below 250 K. Most importantly, however, the observation of a uniformly spaced structure and high conductivity for $[HCN_2S_2]_6[I]_{1.1}$ confirms that a small degree of p-type doping of neutral dithiadiazolyls away from their neutral oxidation state (a half-filled energy band) can generate a room-temperature molecular conductor.

(18) (a) Perlstein, J. H. *Angew. Chem., Int. Ed. Engl.* **1977**, *16*, 519. (b) Foster, R. *Organic Charge Transfer Complexes*; Academic Press: New York, 1969; Chapter 9. (c) Gutmann, F. *Organic Semiconductors*; Wiley: New York, 1967; p 84.

(19) Warmack, R. J.; Callcot, T. A.; Watson, C. R. *Phys. Rev.* **1975**, *B12*, 3336.

(20) If charge transfer from iodine were complete, so that a discrete iodide (rather than intermediate polyiodide) were formed, each ring would carry a charge of +0.18, i.e., 1.1/6.

Table 4. Crystal Data

formula	$S_4N_{4.16}C_2H_2$	$S_2N_2CHI_{0.18}$
fw	212.4	128.20
a, Å	6.816(3)	14.132(16)
b, Å	13.940(2)	14.132(16)
c, Å	14.403(3)	3.352(5)
α, deg	116.830(14)	90
β, deg	98.64(3)	90
γ, deg	99.18(3)	120
V, Å^3	1166.5(6)	579.8(1)
d(calcd), g cm^{-3}	1.81	2.203
space group	$P\bar{1}$	$P6_1$
Z	6	6
λ, Å	0.710 73	0.710 73
temp, K	293	293
μ, mm^{-1}	1.10	2.38
$R(F^2)$, $R_w(F^2)$[a]	0.045, 0.054	0.074, 0.115

[a] $R = [\Sigma||F_o| - |F_c||]/[\Sigma|F_o|]$; $R_w = \{[\Sigma w||F_o| - |F_c||^2]/[\Sigma(w|F_o|^2)]\}^{1/2}$

Starting Materials and General Procedures. Iodine was obtained commercially (Fisher) and used as received. 1,2,3,5-Dithiadiazolyl was prepared as described previously.[10] Sublimations and gas-phase reactions were performed in an ATS Series 3210 three-zone tube furnace, linked to a Series 1400 temperature-control system. Elemental analyses were performed by MHW Laboratories, Phoenix, AZ.

Triclinic Phase of $[HCN_2S_2]_2$. Sublimation of either the triclinic phase of **2** described here or the monoclinic phase reported earlier affords vapors of the radical **1**. In crystal growth experiments the phase of the starting dimer was thus immaterial. Crystals of the triclinic phase were typically (but not exclusively) obtained by sublimation of the crude dimer (prepared as described previously) in a pot sublimer immersed in a warm (30–35 °C) water bath and evacuated to a static vacuum of about 10^{-2} Torr. The sublimate was collected on an ice/water-cooled finger over a period of 24 h. In contrast to the crystals of the monoclinic phase, which are well-faceted, the thin, black needles of the triclinic phase are fibrous and prone to splintering. Cleaving the crystals, for mounting purposes, was therefore difficult.

Iodine-Doped Hexagonal Phase. Crystals of either phase of dimer **2** (usually about 0.5 g), along with iodine (in a ratio of HCN_2S_2:I of 5:1), were sealed at 10^{-3} Torr in a 25 × 250 mm Pyrex tube which was placed in a tube furnace ramped from 70 to 30 °C. Over a period of about 24 h the two reagents vaporized in the warm zone and condensed in the cooler zone. The tube was then inverted and the sublimation cycle repeated. This mixing process was continued until the sublimate exhibited a homogeneous appearance. The doped material grows as long, silver-black rods with lustrous, well-faceted, hexagonal faces. The crystals are both air- and heat-sensitive but can be handled in dry air (for X-ray mounting purposes) for 1–2 min without decomposition. The elemental composition of the material has been established by X-ray crystallography and by numerous elemental (C, H, N, and I) analyses. Two typical analyses (with the formula expressed in terms of the numbers of iodines per six HCN_2S_2 units) are provided.[21] Anal. Calc for $C_6H_6N_{12}S_{12}I_{1.1}$: C, 9.73; H, 0.78; N, 21.81; I, 18.12. Found: (1) C, 9.73; H, 1.31; N, 21.86; I, 17.94; (2) C, 9.31; H, 1.02; N, 21.82; I, 17.97.

X-ray Measurements. All X-ray data were collected on an ENRAF-Nonius CAD-4 diffractometer with monochromated Mo Kα (λ = 0.71073 Å) radiation. Crystals were sealed in epoxy and sealed in glass tubes. Data were collected using a $\theta/2\theta$ technique. The structures were solved using direct methods/SHELX and refined by full-matrix least squares which minimized $\Sigma w(\Delta F)^2$. A summary of crystallographic data is provided in Table 4. Special notes on both structures follow.

Triclinic $[HCN_2S_2]_2$. Like their monoclinic counterparts, crystals of the triclinic phase of $[HCN_2S_2]_2$ readily twin; the data set used for this report is one of two complete data sets collected; sixteen different crystals were actually mounted on the diffractometer in order to find those with minimal twinning. The twinning of the data crystal used (as verified by

(21) For an iodine content of $I_{1.2}$, the percent composition of iodine is calculated to be 19.44. The reported composition of $I_{1.1}$ is based on the statistics of the X-ray refinement and is entirely consistent with the analytical data.

multiple-layer Weissenberg photographs) had overlap of two $0kl$ grids and lattice coincidences for $h = 3$ ($R = 0.55$) and $h = 6$ ($R = 0.52$). Two persistent difference map peaks in the columnar cavity were treated as partial nitrogen atoms; refinement of the occupancy with fixed map positions and isotropic U-values of 0.45 gave occupancies of 0.30 for N98 and 0.15 for N99. The inclusion of these nitrogen atoms lowered the R-factor from 0.050 to 0.045. This significant drop in R and the 1.2-Å spacings suggest the possibility that these atoms represent trapped N_2 molecules. Whether or not this is the case, the inclusion of these atoms in the refinement has a less than 1σ effect on all the structural parameters of the dimer units. The structure appears hexagonal in projection (Figure 1), but the intensity symmetry shows it is not. The most nearly hexagonal cell to which the triclinic cell can be transformed is $24.05 \times 24.15 \times 6.816$ Å^3 with angles of 89.86(3), 89.52(2), and 117.86(1)°, and with this cell the R(merge) is 0.50 with 3480 supposedly equivalent reflections differing by more than 10 σ. It is the x-values (perpendicular to the hexagonal projection) which are not consistent with hexagonal symmetry. It is not apparent why this near-hexagonal structure is preferable to an exact-hexagonal packing.

$[HCN_2S_2]_6[I_{1.1}]$. Twinning problems and the desire to check the reproducibility of the iodine content led to many crystals being examined for this compound. Eighteen crystals were investigated on the diffractometer, and complete data sets were obtained for four different crystals. Each of the four refinements gave total occupancies of 0.18–0.22 I atoms per radical unit for a reasonable range of isotropic U-values for the I atoms. In the refinement of this report, positions of the two iodine fragments were restricted to difference map positions, while the isotropic displacement parameters and the occupancy factors were refined alternately. The difference in the two isotropic U-values for the data set reported here defies rationalization, but the consistency of the iodine content in the four separate refinements provides the desired agreement with the analytical results. We attribute the relatively high final R-value to likely data imperfections arising from twinning and also to inadequacies of our structure to model exactly the disorder of the iodine channel.

Magnetic Measurements. The magnetic susceptibility of $[HCN_2S_2]_6[I_{1.1}]$ was measured from 4.2 to about 400 K by using the Faraday technique. Details of the apparatus have been previously described.[22]

Raman Spectra. Raman spectra were recorded on a Bruker FRA 106 FT Raman module interfaced to a Bruker IFS 66 FTIR bench. For the undoped material, data was accumulated for 200 scans with a laser power of 250 mW. The full spectrum of the undoped material exhibits bands at 3029(m), 1482(w), 1372(w), 1245(w), 779(s), 742(w), 501(w), 462(s), and 124(vs) cm^{-1}. The same number of scans (200) was used for the doped compound (at both 295 and 130 K); slight sample heating (blackbody radiation) required that a lower laser power (70 mW) be used.

Acknowledgment. Financial support at Guelph was provided by the Natural Sciences and Engineering Research Council of Canada (NSERC) and at Arkansas by the National Science Foundation (EPSCOR program). C.D.B. acknowledges a DOE/ASTA Traineeship. We thank Ms. Janice Hellman, of Bruker Spectrospin (Canada) Ltd., for assistance in obtaining the Raman spectra.

Supplementary Material Available: Tables of crystal data, structure solution and refinement, atomic coordinates, bond lengths and angles, and anisotropic thermal parameters, and ORTEP drawings (7 pages). This material is contained in many libraries on microfiche, immediately follows this article in the microfilm versionof the journal, and can be orderedfrom the ACS; see any current masthead page for ordering information.

(22) (a) DiSalvo, F. J.; Waszczak, J. V. *Phys. Rev.* **1981**, *B23*, 457. (b) DiSalvo, F. J.; Waszczak, J. V.; Tauc, J. *Phys. Rev.* **1972**, *B6*, 4574.